

## PREPARATION AND PHYSICO-CHEMICAL PROPERTIES OF LANTHANIDE(III) COMPLEXES WITH 2-((E)-(TERT-BUTYLIMINO)METHYL)-6-METHOXYPHENOL

Kwakhanya Mkwakwi, Eric Hosten, Richard Betz, Abubak'r Abrahams and Tatenda Madanhire\*

Department of Chemistry, Nelson Mandela University, PO Box 77000, 6031 Port Elizabeth, South Africa

(Received August 15, 2022; Revised September 5, 2023; Accepted September 6, 2023)

**ABSTRACT.** The reactions of lanthanide nitrates with 2-((E)-(tert-butylimino)methyl)-6-methoxyphenol (HL<sub>1</sub>) have yielded five complexes that are described by the formulae [Ce(HL<sub>1</sub>)<sub>2</sub>(NO<sub>3</sub>)<sub>3</sub>]·MeOH and [Ln(HL<sub>1</sub>)<sub>2</sub>(NO<sub>3</sub>)<sub>3</sub>] (Ln = Nd(III), Gd(III), Ho(III) and Er(III)) and were characterized using physico-chemical techniques including single-crystal X-ray diffraction spectroscopy. The cerium complex crystallized in a triclinic *P-1* space group, while the rest of the complexes crystallized in the monoclinic *P21/c* space group. All the complexes are ten-coordinate, adopting a tetradehedron geometry with two HL<sub>1</sub> molecules coordinated through the phenolic and methoxy oxygen atoms. The coordination sphere is completed by six oxygen atoms from three bidentately coordinated nitrate ligands. Electronic data reveals that only the neodymium, holmium and erbium complexes exhibit weak *f-f* transitions in the visible region.

**KEY WORDS:** Preparation, Physico-chemical properties, Lanthanide, Schiff base complexes, Crystal structure, Geometry

### INTRODUCTION

Schiff base ligands with oxygen and nitrogen donor atoms in their structures are good chelating agents for transition and non-transition metals, as well as in the preparation of heterometallic 3*d*-4*f* complexes [1-4]. The nitrogen and oxygen donor atoms are suitable for the complexation of transition metal ions, while the oxygen donor atoms prefer oxophilic ions, such as lanthanide ions [4].

Lanthanide complexes with *o*-vanillin Schiff base derivatives have been synthesized and their interesting magnetic and luminescent properties investigated for preparing new materials and ideal probes in biology [4-9]. *o*-Vanillin derived Schiff bases can yield monomeric, dimeric or polymeric metal complexes under various reaction conditions (e.g. varying metal to ligand ratio or solvents), with coordination occurring bidentately (*N,O*- or *O,O*-donor), tridentately (*O,O,N*-donor) or multidentately, as well as adopting bridging modes [7-9]. In dinuclear or polynuclear complexes, bridging between the Ln(III) ions can also be facilitated by co-ligands, such as chloride ions [9]. Furthermore, some *o*-vanillin derived Schiff base ligands are characterized by the migration of the phenolic proton to the azomethine nitrogen to yield a zwitterion [7]. The latter phenomenon was observed in mononuclear La(III) and Nd(III) complexes with the *O,O*-donor *N,N'*-bis(3-methoxysalicylidene)propane-1,2-diamine (H<sub>2</sub>Sal): [La(H<sub>2</sub>Sal)(NO<sub>3</sub>)<sub>3</sub>(MeOH)]·H<sub>2</sub>O and [Nd(H<sub>2</sub>Sal)(NO<sub>3</sub>)<sub>3</sub>] [7].

An ion-pair uniting gadolinium(III) with the potentially *O,N,O*-donor ligand 2-((E)-(tert-butylimino)methyl)-6-methoxyphenol (HL<sub>1</sub>, Figure 1) and uranyl tetrachloride, as depicted in Figure 2, was reported by Moll *et al.* [10]. The ion-pair consists of two [GdCl<sub>2</sub>(HL<sub>1</sub>)<sub>2</sub>(py)<sub>2</sub>]<sup>+</sup> complexes countered by one uranyl tetrachloride. The gadolinium ion formed an eight-coordinate complex, which consisted of two bidentately coordinated *O,O*-donor Schiff base ligands bound to the metal ion through their methoxy and phenoxide oxygens, two pyridine nitrogens and two

\*Corresponding author. E-mail: Tatenda.Madhanhire@mandela.ac.za

This work is licensed under the Creative Commons Attribution 4.0 International License

chlorides. The Gd-O bond lengths range from 2.298-2.61 Å, the Gd-Cl bond lengths are 2.6695 and 2.6869 Å, and the average Gd-N bond distance is 2.6145 Å.

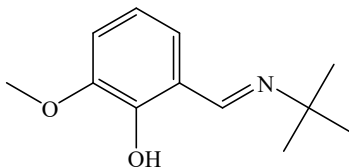


Figure 1. The chemical structure of HL1.

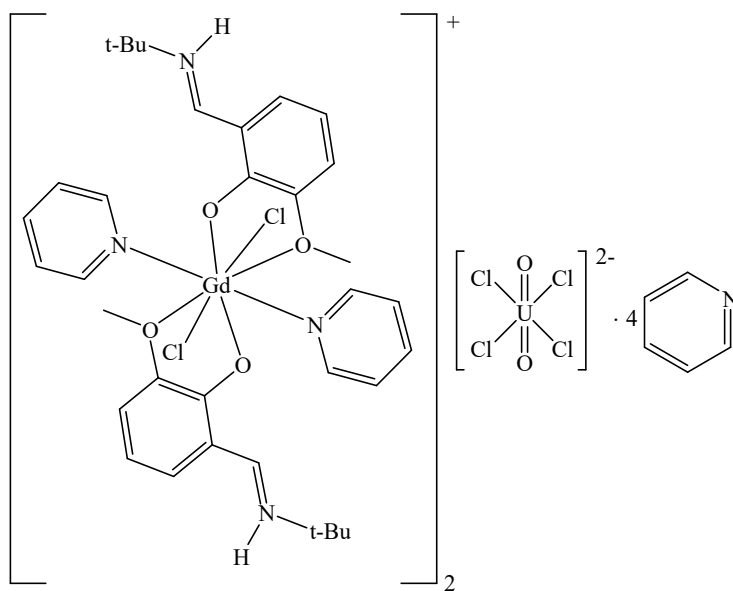


Figure 2. The structural representation of the gadolinium(III)-Schiff base complex and uranyl tetrachloride.

To further explore the coordination behaviour of HL<sub>1</sub>, we have prepared and characterized five lanthanide complexes with the general formulae [Ce(HL<sub>1</sub>)<sub>2</sub>(NO<sub>3</sub>)<sub>3</sub>]·MeOH and [Ln(HL<sub>1</sub>)<sub>2</sub>(NO<sub>3</sub>)<sub>3</sub>] (Ln = Nd, Gd, Ho and Er).

## EXPERIMENTAL

### *Materials and physical measurements*

The following organic solvents were used in the study: methanol, ethanol, dimethyl formamide, pyridine and diethyl ether. Dimethyl formamide was purchased from Sigma-Aldrich, while all the other solvents were sourced from Merck and used without further purification. The deuterated solvents utilized in NMR spectroscopy, CDCl<sub>3</sub> and DMSO-*d*<sub>6</sub> were obtained from Merck. The lanthanide nitrates, Ln(NO<sub>3</sub>)<sub>3</sub>·*x*H<sub>2</sub>O (Ln = Ce, Nd, Gd, Ho and Er; *x* = 6 for Ce, Nd and Gd; *x* = 5 for Ho and Er) with 99.9% purity were sourced from Sigma-Aldrich. *o*-Vanillin (99.0%) and *tert*-

butylamine (99.0%) used in the preparation of the organic ligand were purchased from Sigma-Aldrich and Riedel-de Haën, respectively, and used as supplied.

A Bruker Tensor 27 FT-IR spectrophotometer (equipped with the Platinum ATR attachment) was utilized to obtain the infrared spectra of all the compounds synthesized in this study. The samples were run neat on ATR and the data recorded and analysed with *OPUS 6.5* software. The UV-Vis spectra were carried out on a PerkinElmer Lambda 35 UV-Vis spectrophotometer and processing done using *UV WinLab* software. Nuclear Magnetic Resonance (NMR) spectra were recorded at 295K using a Bruker AvanceIII 400 NMR Spectrometer and acquisition done using *TopSpin 3.0* software. Analysis of the NMR spectra was performed using *ACD/Labs* software.

Table 1. Crystal and structure refinement data for complexes 1–5.

Complex	1	2	3	4	5
Formula	2(C <sub>24</sub> H <sub>34</sub> CeN <sub>5</sub> O <sub>13</sub> ), CH <sub>4</sub> O	C <sub>24</sub> H <sub>34</sub> N <sub>5</sub> NdO <sub>13</sub>	C <sub>24</sub> H <sub>34</sub> GdN <sub>5</sub> O <sub>13</sub>	C <sub>24</sub> H <sub>34</sub> HoN <sub>5</sub> O <sub>13</sub>	C <sub>24</sub> H <sub>34</sub> N <sub>5</sub> ErO <sub>13</sub>
M <sub>r</sub> (g.mol <sup>-1</sup> )	1513.41	744.80	757.81	765.49	767.82
Crystal system	Triclinic	Monoclinic	Monoclinic	Monoclinic	Monoclinic
Space group	<i>P</i> -1 (No. 2)	<i>P</i> 2 <sub>1</sub> / <i>c</i> (No. 14)			
a (Å)	9.4495(7)	11.8651(6)	11.8855(8)	11.9289(6)	11.9366(4)
b (Å)	12.0101(8)	12.9123(6)	12.8089(9)	12.7376(6)	12.7330(5)
c (Å)	15.6454(10)	20.4752(10)	20.3474(13)	20.2845(10)	20.2595(6)
α (°)	91.652(3)	90	90	90	90
β (°)	91.652(3)	78.014(2)	91.015(3)	78.748(2)	90.650(1)
γ (°)	110.041(2)	90	90	90	90
V (Å <sup>3</sup> )	1595.59(19)	3136.1(3)	3097.2(4)	3081.9(3)	3079.02(18)
Z	1	4	4	4	4
ρ (g.cm <sup>-3</sup> )	1.575	1.577	1.625	1.650	1.656
μ (mm <sup>-1</sup> )	1.497	1.724	2.211	2.637	2.795
F(000)	768	1508	1524	1536	1540
Crystal size (mm <sup>3</sup> )	0.14 x 0.26 x 0.36	0.17 x 0.26 x 0.44	0.39 x 0.57 x 0.64	0.16 x 0.24 x 0.36	0.27 x 0.31 x 0.53
θ (min-max) (°)	1.9, 28.3	1.9, 28.3	1.9, 28.3	1.9, 28.4	1.9, 28.3
Data set	-12 ≤ h ≤ 12 -15 ≤ k ≤ 15 -20 ≤ l ≤ 20	-15 ≤ h ≤ 15 -17 ≤ k ≤ 17 -22 ≤ l ≤ 27	-14 ≤ h ≤ 15 -17 ≤ k ≤ 15 -27 ≤ l ≤ 27	-15 ≤ h ≤ 15 -17 ≤ k ≤ 16 -24 ≤ l ≤ 27	-15 ≤ h ≤ 15 -14 ≤ k ≤ 17 -27 ≤ l ≤ 26
Tot., Unique data, R <sub>int</sub>	29288, 7907, 0.014	45146, 7803, 0.017	56688, 7696, 0.020	30338, 7676, 0.022	26574, 7632, 0.014
Observed [I > 2σ(I)] reflections	7430	6733	6594	6356	6545
N <sub>reflections</sub> , N <sub>parameters</sub>	7907, 445	7803, 404	7696, 404	7676, 404	7632, 404
R[F <sup>2</sup> > 2σ(F <sup>2</sup> )], wR(F <sup>2</sup> ), S	0.0194, 0.0499, 1.06	0.0224, 0.0553, 1.08	0.0272, 0.0585, 1.27	0.0212, 0.0502, 1.02	0.0239, 0.0551, 1.20
Δρ <sub>min</sub> , Δρ <sub>max</sub> (e.Å <sup>-3</sup> )	-0.48, 0.68	-0.45, 0.97	-1.00, 1.69	-0.56, 0.71	-0.97, 1.46

A Bruker APEX II CCD diffractometer was used to record X-ray crystallographic data. The data reduction and cell refinement were done using *SAINTE* software [11]. The crystal structures were solved and refined using *SHELXS97* and *SHELXL97* software, respectively [12, 13]. Molecular graphics were obtained using *ORTEP-3* [14] and *Mercury* [15]. The coordination geometries of

the lanthanide complexes were analysed using *SHAPE 2.1* software. A summary of the crystal data and parameters for data collection and refinement for complexes **1–5** is shown in Table 1.

*Synthesis of 2-((E)-(tert-butylimino)methyl)-6-methoxyphenol (HL<sub>1</sub>)*

The preparation of HL<sub>1</sub> was carried out by dissolving (1.47 g, 20 mmol) of *tert*-butylamine in 20 mL of methanol. The resulting solution was added to a stirred solution of *o*-vanillin (3.04 g, 20 mmol) in 20 mL of methanol at room temperature. The colour of the solution changed from light yellow to intense yellow immediately. The solution was refluxed for 1 h before the solvent was reduced to 5 mL using a rotary evaporator. The resulting yellow crystals were washed with diethyl ether and dried in vacuum overnight. Yield: 3.8325 g (92.0 %), m.p. = 88.9 °C. UV-Vis (DMF,  $\lambda_{\max}$  nm ( $\epsilon$ , M<sup>-1</sup> cm<sup>-1</sup>)): 268 (30778), 332 (9880), 416 (2110). IR (cm<sup>-1</sup>):  $\nu$ (C-H) 2967, 2963, 2904(w);  $\nu$ (-OCH<sub>3</sub>) 2837(w);  $\nu$ (C=N) 1626(s);  $\nu$ (C<sub>ph</sub>-O) 1251(s). <sup>1</sup>H NMR (CDCl<sub>3</sub>,  $\delta$  ppm): 8.26 (s, 1H, C=N), 6.85 (s, 2H, Ar), 6.72-6.68 (t, 1H, Ar), 3.89 (s, 1H, -OH), 3.86 (s, 3H, -OCH<sub>3</sub>), 1.33 (s, 9H, -CH<sub>3</sub>).

*Synthesis of metal complexes 1–5*

A solution of Ln(NO<sub>3</sub>)<sub>3</sub>·xH<sub>2</sub>O (0.5 mmol) in 10 mL of methanol was added to a methanolic solution of HL<sub>1</sub> (1.5 mmol). The resulting yellow solution was kept at room temperature and single crystals suitable for X-ray crystallography were obtained within 24 h from the mother liquor.

*Synthesis of bis(2-((E)-(tert-butylimino)methyl)-6-methoxyphenol)trinitrato cerium(III) methanol, [Ce(NO<sub>3</sub>)<sub>3</sub>(HL<sub>1</sub>)<sub>2</sub>]·MeOH (1).* Ce(NO<sub>3</sub>)<sub>3</sub>·6H<sub>2</sub>O (0.217 g, 0.5 mmol), HL<sub>1</sub> (0.312 g, 1.5 mmol). Red crystals, yield = 0.08168 g (10.8%, based on Ce), m.p. = 150 °C. Anal. calc. for C<sub>49</sub>H<sub>82</sub>CeN<sub>10</sub>O<sub>24</sub> (%): C, 38.89; H, 4.80; N, 9.26. Found: C, 39.40; H, 4.65; N, 8.90. Conductivity (10<sup>-3</sup> M, DMF): 160.7 ohm<sup>-1</sup>cm<sup>2</sup>mol<sup>-1</sup>. UV-Vis (DMF,  $\lambda_{\max}$  nm ( $\epsilon$ , M<sup>-1</sup>cm<sup>-1</sup>)): 268 (17420), 335 (5584), 402 (1798). IR (cm<sup>-1</sup>):  $\nu$ (C-H) 2980(w);  $\nu$ (C=N) 1645(s);  $\nu_1$ (NO<sub>3</sub><sup>-</sup>) 1294(s);  $\nu_4$ (NO<sub>3</sub><sup>-</sup>) 1453(w);  $\nu_2$ (NO<sub>3</sub><sup>-</sup>) 1032(m);  $\nu_6$ (NO<sub>3</sub><sup>-</sup>) 818(w);  $\nu$ (Ce-O) 411(w).

*Synthesis of bis(2-((E)-(tert-butylimino)methyl)-6-methoxyphenol)trinitrato neodymium(III), [Nd(NO<sub>3</sub>)<sub>3</sub>(HL<sub>1</sub>)<sub>2</sub>] (2).* Nd(NO<sub>3</sub>)<sub>3</sub>·6H<sub>2</sub>O (0.219 g, 0.5 mmol), HL<sub>1</sub> (0.312 g, 1.5 mmol). Lime green crystals, yield = 0.1604 g (43.1%, based on Nd), m.p. = 212 °C. Anal. calc. for C<sub>24</sub>H<sub>34</sub>NdN<sub>5</sub>O<sub>13</sub> (%): C, 38.70; H, 4.60; N, 9.40. Found: C, 38.74; H, 4.54; N, 9.01. Conductivity (10<sup>-3</sup> M, DMF): 96 ohm<sup>-1</sup>cm<sup>2</sup>mol<sup>-1</sup>. UV-Vis (DMF,  $\lambda_{\max}$  nm ( $\epsilon$ , M<sup>-1</sup>cm<sup>-1</sup>)): 268 (15850), 336 (4588), 415 (1480), 517 (22.5), 524 (24.1), 582 (30.2), 735 (17.5), 749 (17.4) 799 (23.8). IR (cm<sup>-1</sup>):  $\nu$ (C-H) 2976(w);  $\nu$ (C=N) 1639 (s);  $\nu_1$ (NO<sub>3</sub><sup>-</sup>) 1295(s);  $\nu_4$ (NO<sub>3</sub><sup>-</sup>) 1478(s);  $\nu_2$ (NO<sub>3</sub><sup>-</sup>) 1031(m);  $\nu_6$ (NO<sub>3</sub><sup>-</sup>) 817(w);  $\nu$ (Nd-O) 411(w).

*Synthesis of bis(2-((E)-(tert-butylimino)methyl)-6-methoxyphenol)trinitrato gadolinium(III), [Gd(NO<sub>3</sub>)<sub>3</sub>(HL<sub>1</sub>)<sub>2</sub>] (3).* Gd(NO<sub>3</sub>)<sub>3</sub>·6H<sub>2</sub>O (0.226 g, 0.5 mmol), HL<sub>1</sub> (0.315 g, 1.5 mmol). Yellow crystals, yield: 0.1632 g (43.0%, based on Gd), m.p. = 212 °C. Conductivity (10<sup>-3</sup> M, DMF): 120.6 ohm<sup>-1</sup>cm<sup>2</sup>mol<sup>-1</sup>. UV-Vis (DMF,  $\lambda_{\max}$  nm ( $\epsilon$ , M<sup>-1</sup>cm<sup>-1</sup>)): 268 (17138), 334 (5144), 411 (1780). IR (cm<sup>-1</sup>):  $\nu$ (C-H) 2975(w);  $\nu$ (C=N) 1638(s);  $\nu_1$ (NO<sub>3</sub><sup>-</sup>) 1299(s);  $\nu_4$ (NO<sub>3</sub><sup>-</sup>) 1475(s);  $\nu_2$ (NO<sub>3</sub><sup>-</sup>) 1034(m);  $\nu_6$ (NO<sub>3</sub><sup>-</sup>) 817(w);  $\nu$ (Gd-O) 416(w).

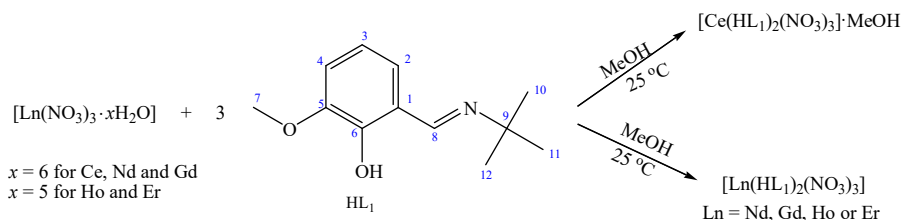
*Synthesis of bis(2-((E)-(tert-butylimino)methyl)-6-methoxyphenol)trinitrato holmium(III), [Ho(NO<sub>3</sub>)<sub>3</sub>(HL<sub>1</sub>)<sub>2</sub>] (4).* Ho(NO<sub>3</sub>)<sub>3</sub>·5H<sub>2</sub>O (0.221 g, 0.5 mmol), HL<sub>1</sub> (0.315 g, 1.5 mmol). Yellow crystals, yield = 0.1676 g (43.7%, based on Ho), m.p. = 198.4 °C. Anal. calc. for C<sub>24</sub>H<sub>34</sub>HoN<sub>5</sub>O<sub>13</sub> (%): C, 37.66; H, 4.48; N, 9.15. Found: C, 37.58; H, 4.54; N, 8.82. Conductivity (10<sup>-3</sup> M, DMF): 130.6 ohm<sup>-1</sup>cm<sup>2</sup>mol<sup>-1</sup>. UV-Vis (DMF,  $\lambda_{\max}$  nm ( $\epsilon$ , M<sup>-1</sup>cm<sup>-1</sup>)): 267 (16530), 328 (5158), 415 (1582),

539 (25.7), 641 (17.8). IR ( $\text{cm}^{-1}$ ):  $\nu(\text{C-H})$  2979(w);  $\nu(\text{C=N})$  1641(m);  $\nu_1(\text{NO}_3^-)$  1304(s),  $\nu_4(\text{NO}_3^-)$  1471(s);  $\nu_2(\text{NO}_3^-)$  1037(m);  $\nu_6(\text{NO}_3^-)$  817(w);  $\nu(\text{Ce-O})$  411(w).

*Synthesis of bis(2-((E)-(tert-butylimino)methyl)-6-methoxyphenol)trinitrato erbium(III), [Er(NO<sub>3</sub>)<sub>3</sub>(HL<sub>1</sub>)<sub>2</sub>] (5).* Er(NO<sub>3</sub>)<sub>3</sub>·5H<sub>2</sub>O (0.222 g, 0.5 mmol) and HL<sub>1</sub> (0.312 g, 1.5 mmol). Yellow crystals, yield = 0.1446 g (37.6%, based on Er), m.p. = 212 °C. Anal. calc. for C<sub>24</sub>H<sub>34</sub>ErN<sub>5</sub>O<sub>13</sub> (%): C, 37.54; H, 4.46; N, 9.12. Found: C, 37.43; H, 4.42; N, 8.97. Conductivity (10<sup>-3</sup> M, DMF): 112.7 ohm<sup>-1</sup>cm<sup>2</sup>mol<sup>-1</sup>. UV-Vis (DMF,  $\lambda_{\text{max}}$  nm ( $\epsilon$ , M<sup>-1</sup>cm<sup>-1</sup>)): 268 (17472), 328 (5404), 415 (1672), 519 (29.5), 542 (20), 655 (16.3). IR ( $\text{cm}^{-1}$ ):  $\nu(\text{C-H})$  2978(w);  $\nu(\text{C=N})$  1638(s);  $\nu_1(\text{NO}_3^-)$  1303(s);  $\nu_4(\text{NO}_3^-)$  1471(s);  $\nu_2(\text{NO}_3^-)$  1036(m);  $\nu_6(\text{NO}_3^-)$  817(w);  $\nu(\text{Ce-O})$  420(w).

## RESULTS AND DISCUSSION

Complexes **1-5** were synthesized by the reaction of three equivalents of HL<sub>1</sub> with lanthanide nitrate salts in methanol (Scheme 1). The resulting mixtures were kept at room temperature and single crystals formed after 24 hours.



Scheme 1. General synthetic protocol for complexes **1-5**, with atom numbering scheme for the ligand.

All the complexes were found to be stable in air for months, are non-hygroscopic and readily dissolved in DMF, DMSO and pyridine. However, they were partially soluble in both hot and cold methanol and ethanol. The complexes were found to be insoluble in acetonitrile, chloroform, chlorobenzene, diethyl ether, dichloromethane, isopropyl alcohol and water.

The molar conductivity of 10<sup>-3</sup> M solutions of the rare-earth complexes in DMF were measured at ambient temperature. The molar conductivity of **1** and **4** is 160.7 and 130.6 ohm<sup>-1</sup>cm<sup>2</sup>mol<sup>-1</sup>, respectively, which fall within the 2:1 electrolyte type range [16]. The conductivity of complexes **2**, **3** and **5** are 96.0, 120.6 and 212.0 ohm<sup>-1</sup>cm<sup>2</sup>mol<sup>-1</sup>, respectively. These values fall outside both the 1:1 and 2:1 electrolyte type ranges.

### IR and NMR spectroscopy

The IR spectra of HL<sub>1</sub> exhibited a series of weak bands from 2967 to 2907 cm<sup>-1</sup>, which are due to the C-H stretching vibrations. The weak intensity band at 2837 cm<sup>-1</sup> is attributed to the  $\nu(-\text{OCH}_3)$ , while the strong intensity band at 1626 cm<sup>-1</sup> is attributed to the azomethine absorption. The stretching frequency at 1251 cm<sup>-1</sup> arises from the C-O vibration of the phenol group.

Upon coordination to the metal, most of the ligand's C-H band intensities are reduced significantly except for the stretching vibration at about 2978 cm<sup>-1</sup> which has shifted to a higher frequency compared to the free ligand. The C=N stretching frequency, which was observed at 1641 cm<sup>-1</sup> in the free ligand, has shifted to a higher wavenumber by approximately 15 cm<sup>-1</sup> upon coordination. The three bands near 1453 cm<sup>-1</sup> ( $\nu_4$ ), and those at 1294 cm<sup>-1</sup> ( $\nu_1$ ), 1037 cm<sup>-1</sup> ( $\nu_2$ ) and 817 cm<sup>-1</sup> ( $\nu_6$ ) can be attributed to the coordinated nitrate ions [17]. The difference between the

peak positions of  $\nu_4$  and  $\nu_1$  is  $209\text{ cm}^{-1}$  which is indicative of bidentately coordinated nitrates [4, 18]. Coordination of the phenolic oxygen was confirmed by the blue shift of the C-O vibration frequency from  $1251$  to about  $1299\text{ cm}^{-1}$ . The  $\nu(\text{Ln-O})$  band in the complexes ranges from  $411$  to  $420\text{ cm}^{-1}$  [19].

The  $^1\text{H}$  and  $^{13}\text{C}$  NMR spectra of  $\text{HL}_1$  were recorded in  $\text{CDCl}_3$  and  $\text{DMSO-}d_6$ , respectively. The peak at  $8.26\text{ ppm}$  is assigned to proton 8 of the azomethine (C=N) group. The doublet at  $6.84\text{ ppm}$  integrating to two protons is attributed to protons 2 and 4 of the benzene ring. The triplet between  $6.72$ - $6.68\text{ ppm}$  is due to the resonance of proton 3. The phenolic proton resonates as a singlet at  $3.88\text{ ppm}$ . The peak at  $3.86\text{ ppm}$  is assigned to the three *o*-vanillin protons. The singlet peak at  $1.33\text{ ppm}$  is attributed to the *tert*-butyl protons.

Complexes **1-5** exhibit similar  $^1\text{H}$  NMR spectra, each containing a broad peak at approximately  $14.67\text{ ppm}$  which was attributed to the N-H resonance of the zwitterion proton. The resonance of proton H8 is observed at about  $8.58$ - $8.54\text{ ppm}$  which is a downfield shift compared to the free ligand ( $8.26\text{ ppm}$ ). The chemical shift of H2 and H4 in **2**, **4** and **5** appear at  $7.02$ ,  $7.04$  and  $7.04\text{ ppm}$ , respectively, as a broad singlet. In complexes **1** and **3**, the resonance of protons H2 and H4 appears as triplets between  $7.05$ - $6.96$  and  $7.06$ - $6.97\text{ ppm}$ , respectively. In complexes **1** and **3**, the aromatic proton H3 appears as doublet at about  $6.73\text{ ppm}$ , and in complexes **2**, **4** and **5**, proton H3 appears as a singlet at about  $6.74\text{ ppm}$ . It was also noted that the aromatic protons H2, H4 and H3 shifted down-field upon coordination of the ligand. The absence of the phenolic proton signal at  $\sim 3.89\text{ ppm}$  in **1-5** confirms the zwitterionic nature, and subsequent coordination of the ligand. In all the complexes, the singlet observed at about  $3.75\text{ ppm}$  is assigned to the resonance of the methoxy protons; the up-field shift of these protons is attributed to the coordination to the paramagnetic Ln(III) ions. This is caused by the pseudocontact shift as the result of a through-space dipolar interaction between the magnetic moments of the metal ion and the methoxy protons [20]. The chemical shift of the *tert*-butyl protons is identical to that of the free ligand.

The NMR analysis of the compound reveals several key chemical shifts for different carbon atoms. The imine group carbon atom (-C=N-) shows a chemical shift of  $161.75\text{ ppm}$ . The aromatic carbons (C1-C6) exhibit chemical shifts ranging from  $117.08$  to  $154.44\text{ ppm}$ . The carbon atom of the methoxy group is observed at a chemical shift of  $56.25\text{ ppm}$ , while C9 is found at a slightly higher chemical shift of  $56.83\text{ ppm}$ , likely due to its proximity to the imine group. The methyl group carbons (C10-C12) belonging to the butyl moiety display a chemical shift of  $29.75\text{ ppm}$ .

#### Electronic spectroscopy

The electronic spectra of a  $0.05\text{ mM}$  DMF solution of the  $\text{HL}_1$  ligand and complexes were recorded, with the UV-Vis spectrum of the free ligand showing three main maxima at  $268$ ,  $332$  and  $416\text{ nm}$ , which are attributed to  $\pi \rightarrow \pi^*$  transitions of the aromatic ring and the imine group (Figure 3a). The spectrum of **1** reveals no net change to the peak at  $268\text{ nm}$ , while at  $335$  and  $402\text{ nm}$  a red and blue shift is observed, respectively. The electronic spectra of **2-5** are similar, with the average absorption maxima being  $268$ ,  $332$  and  $414\text{ nm}$ . The slight shifts in the maxima could be attributed to the changes in the energy levels of the ligand orbitals upon complexation [4].

The spectra of  $1\text{ mM}$  DMF solutions of complexes **2**, **4** and **5** display weak absorption maxima in the visible region, which are characteristic of Laporte forbidden  $f-f$  transitions, as depicted in Figure 3b. The six bands in the visible region of **2** were shifted to longer wavelengths compared to the free aqua complex (see Table 2) - this shift is due to the nephelauxetic effect [21-23]. The red shift is accepted as an indication of a higher degree of covalency in the compound of interest compared to its aqua compound [24]. The  $f-f$  transitions in complex **4** shifted to shorter wavelength relative to the literature values. The following transitions in complex **5** experienced no significant shifts:  $^4I_{15/2} \rightarrow ^4H_{9/2}$  and  $^4I_{15/2} \rightarrow ^4S_{3/2}$ . However, the transition  $^4I_{15/2} \rightarrow ^2H_{11/2}$  showed a blue shift compared to the free  $\text{Ln}^{3+}$  ions in water.

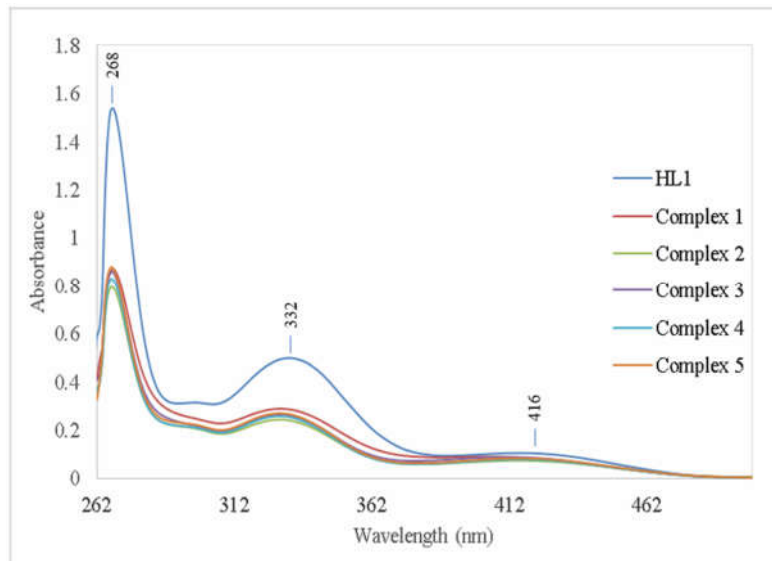


Figure 3a. Overlay UV-Vis spectra of HL<sub>1</sub> and complexes 1-5.

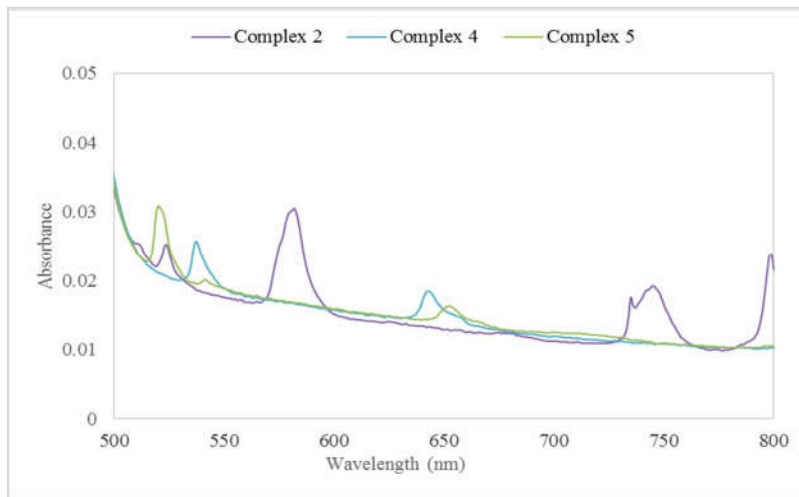
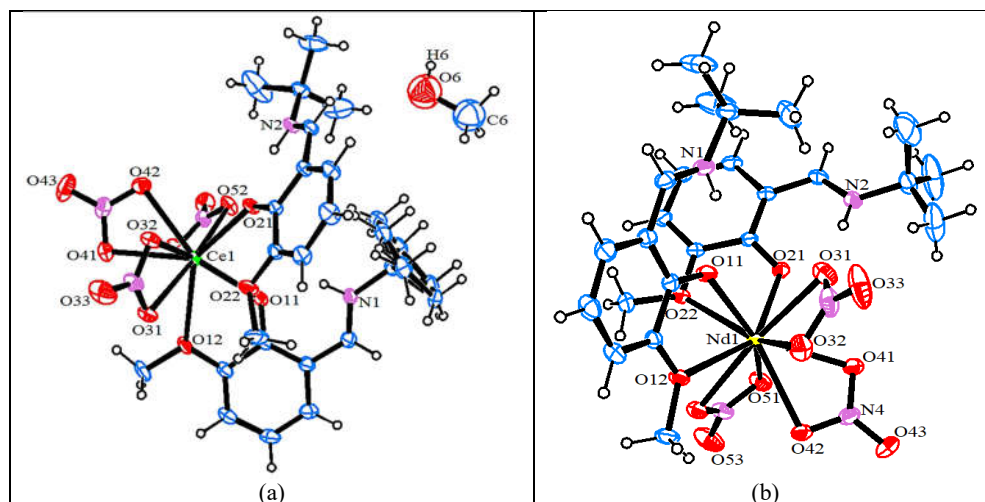


Figure 3b. Visible spectra of  $10^{-3}$  M solutions of HL<sub>1</sub> and complexes 2, 4 and 5 (complexes 1 and 3 exhibit no  $f-f$  transitions and are excluded from the plot).

Table 2.  $4f-4f$  transitions of complexes **2**, **4** and **5**.

Complex	Wavelength (nm)		Assignments
	Experimental	Free Ln <sup>3+</sup> in water [19]	
<b>2</b>	799	794	$^4I_{9/2} \rightarrow ^2H_{9/2}$
	749	740	$\rightarrow ^4S_{3/2}$
	735	732	$\rightarrow ^4F_{7/2}$
	582	576	$\rightarrow ^4G_{5/2}$
	524	521	$\rightarrow ^4G_{7/2}$
	517	512	$\rightarrow ^4D_{3/2}$
<b>4</b>	641	656	$^5H_8 \rightarrow ^5F_5$
	539	544	$\rightarrow ^5F_4$
<b>5</b>	652	652	$^4I_{5/2} \rightarrow ^4H_{9/2}$
	542	541	$\rightarrow ^4S_{3/2}$
	519	523	$\rightarrow ^2H_{11/2}$

Figure 4. The crystal structures of (a) complex **1** and (b) **2** showing 30% probability displacement ellipsoids and partial atom-labelling.

#### *X-ray crystallography*

Complex **1** crystallized in a triclinic ( $P-1$ ) space group, while the isostructural complexes **2-5** crystallized in the monoclinic ( $P21/c$ ) space group. Single-crystal X-ray diffraction data reveals that all the ten-coordinate complexes have identical primary coordination spheres composed of two bidentately coordinated HL<sub>1</sub> molecules which are bonded through the phenolic and methoxide oxygens, and also three bidentately coordinated nitrates (Figures 4a and 4b). The Ce(III) complex is distinguished from **2-5** by possessing one crystallographic methanol molecule. The geometry around the metal centers were analysed using *SHAPE 2.1* [25]. The preferred geometry for all the complexes is distorted tetradecahedron (TD-10) which is characterized by  $12_3+2_4$  faces, 22 edges and  $D_{2d}$  symmetry (Figure 4c) [26]. Figure 4d illustrates the relationship between the continuous

shape measurement (CShM) values of TD-10 geometry and the ionic radii of the lanthanides. It can be seen that there is a decrease in CShM values as the ionic radii decreases from Ce(III) to Er(III) due to decreased room for angular distortions and stronger metal-ligand binding as the metal ions get smaller [27]. This trend reveals that the heavier lanthanide ions prefer the tetradecahedron geometry compared to the earlier ions.

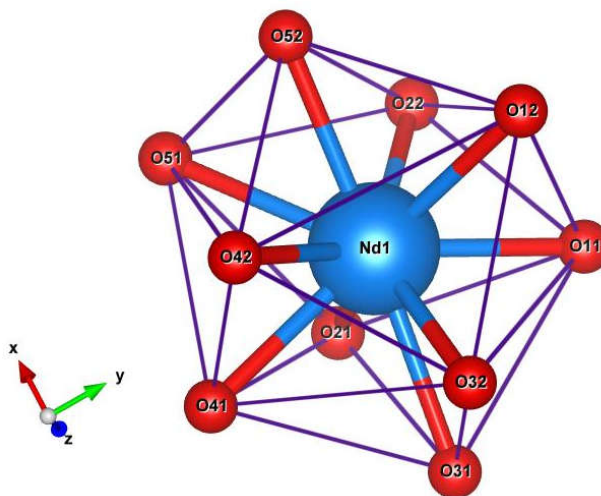
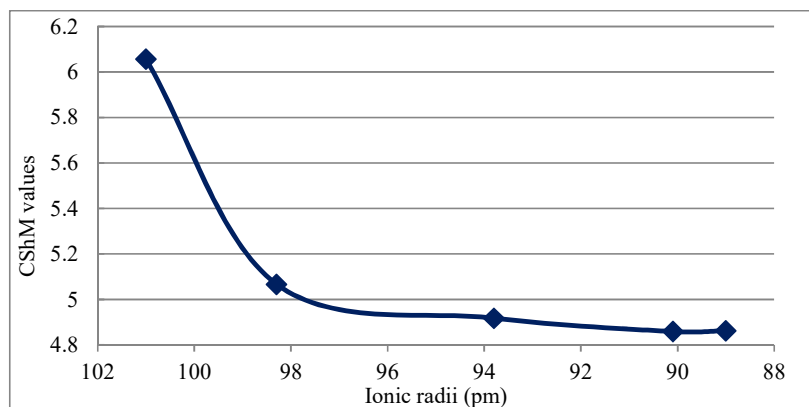


Figure 4c. The distorted polyhedral representation of the tetradecahedron geometry (complex **2**), generated by *VESTA*.

Bond parameters of the metal complexes are gathered in Table 3a. The average bond lengths of the Ln-O<sub>(phenolate)</sub> and Ln-O<sub>(methoxide)</sub> are 2.329 and 2.648 Å, respectively. The Ln-O<sub>(nitrate)</sub> bond distances lie between 2.4190(2)-2.6233(15) Å in **1-5**. It was observed that the Ln-O<sub>(phenolate)</sub> bond length is relatively shorter than the Ln-O<sub>(methoxide)</sub>. This can be attributed to the fact that the phenolate oxygen has a higher electronegativity compared to the methoxide oxygen, and thus a greater attraction exists between the phenolate oxygen and the metal ion, which consequentially leads to a shorter bond length. All the observed Ln-O bond lengths lie within the range of the literature values reported for similar complexes containing bidentate *O,O*-donor ligands (Ln-O<sub>(phenolate)</sub>, Ln-O<sub>(methoxide)</sub> and Ln-O<sub>(nitrate)</sub> varies from 2.2257-2.726 Å) [28, 29]. Upon coordination of the ligand, keto-enol tautomerism occurred in which the phenolic proton migrated to the imino nitrogen. The positively charged C=N-H<sup>+</sup> group is countered by the negative charge on the phenolate ring. The double bond nature of the azomethine (C=N) and phenolate (O=C) groups are confirmed by bond lengths of 1.288 and 1.305 Å, respectively. These bond lengths compare well with similar lanthanide complexes containing ligands displaying keto-enol tautomerism [30]. The N1-C12-C111 bond angle of 123.47(1)° supports the *sp*<sup>2</sup> hybridization of C12. The C3-C4 and C5-C6 bond distances are 1.374 and 1.369 Å, respectively, suggesting the presence of a double bond. The latter is comparable to the literature value (average C-C bond length = 1.364 Å) [31]. Thus, the crystallographic data supports the ketonic form present in the complexes.

Figure 4d. The plot of CShM-value *versus* ionic radii of the lanthanide ions.Table 3a. Selected bond distances (Å) and angles ( $^{\circ}$ ) in complexes 1-5.

	1 [Ce]	2 [Nd]	3 [Gd]	4 [Ho]	5 [Er]
Bond lengths (Å)					
Ln-O11	2.3865(14)	2.3693(16)	2.318(2)	2.2467(15)	2.2368(17)
Ln-O12	2.7055(13)	2.6352(16)	2.5833(19)	2.5781(17)	2.574(2)
Ln-O21	2.3527(12)	2.3320(15)	2.2836(17)	2.2813(16)	2.2715(19)
Ln-O22	2.7501(14)	2.6429(16)	2.599(2)	2.5520(16)	2.5451(19)
Ln-O31	2.5935(15)	2.595(2)	2.501(2)	2.4716(18)	2.463(2)
Ln-O32	2.6173(13)	2.5252(19)	2.507(2)	2.4723(19)	2.463(2)
Ln-O41	2.5849(15)	2.5632(17)	2.511(2)	2.4773(17)	2.4661(19)
Ln-O42	2.6030(15)	2.5598(15)	2.503(2)	2.4635(17)	2.449(2)
Ln-O51	2.5794(16)	2.5661(18)	2.574(2)	2.432(2)	2.419(2)
Ln-O52	2.6233(15)	2.5444(17)	2.470(2)	2.568(2)	2.571(2)
Bond angles ( $^{\circ}$ )					
O11-Ln-O12	60.89(4)	62.32(5)	63.59(6)	65.18(6)	65.43(6)
O21-Ln-O22	60.98(4)	63.36(5)	64.56(7)	64.46(5)	64.70(6)
O31-Ln-O32	48.97(4)	49.81(7)	51.09(7)	51.64(6)	51.83(7)
O41-Ln-O42	49.26(5)	49.95(5)	50.92(7)	51.88(6)	52.10(7)
O51-Ln-O52	48.72(5)	49.91(5)	50.55(8)	50.86(7)	50.92(8)

Figure 4e illustrates the effect of the lanthanide contraction on the average Ln-O<sub>(phenolate)</sub>, Ln-O<sub>(methoxide)</sub> and Ln-O<sub>(nitrate)</sub> bond distances when traversing from Ce to Er. It is expected that the bond distance will gradually decrease as the ionic radius decreases due to the lanthanide. This contraction is attributed to the ineffective screening of the nucleus by the 4*f* electrons, leading to a stronger attraction of the nucleus to the electrons in the outermost shell as the nuclear charge increases. The net result is contraction in the atomic radius [32]. The average Ln-O<sub>(nitrate)</sub> bond distance steadily decreases and, except for the slight deviations in the Ho-O bond length, both the Ln-O<sub>(phenoxide)</sub> and the Ln-O<sub>(methoxide)</sub> distances gradually decrease from Ce to Er. The graph also reveals that, on average, the Ln-O<sub>(phenoxide)</sub> bond length is shorter than both the Ln-O<sub>(methoxide)</sub> and the Ln-O<sub>(nitrate)</sub> lengths. It is worth noting that the (O-Ln-O)<sub>HL1</sub> and (O-Ln-O)<sub>nitrate</sub> bond angles lie in the ranges 60.89(4)–65.43(6) $^{\circ}$  and 48.72–52.10 $^{\circ}$ , respectively, and these bond angles gradually increase as the ionic radius decrease. The observed (O-Ln-O)<sub>HL1</sub> and (O-Ln-O)<sub>nitrate</sub> angles are similar to those found in the literature (55.71–64.51 $^{\circ}$  and 47.6–51.07 $^{\circ}$ , respectively) [28, 29, 32,

33]. The nitrate bite angles are less than that of the *o*-vanillin groups, which is due to the fact that the bidentately coordinated nitrate and the *o*-vanillin groups form four- and five-membered rings, respectively.

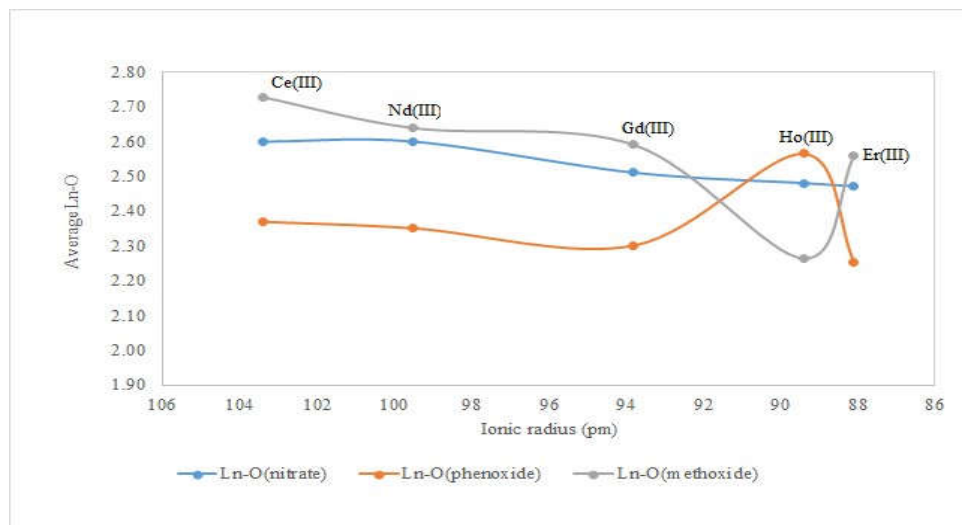


Figure 4e. The plot of the average Ln-O bond lengths in complexes 1-5 versus the lanthanide ionic radius.

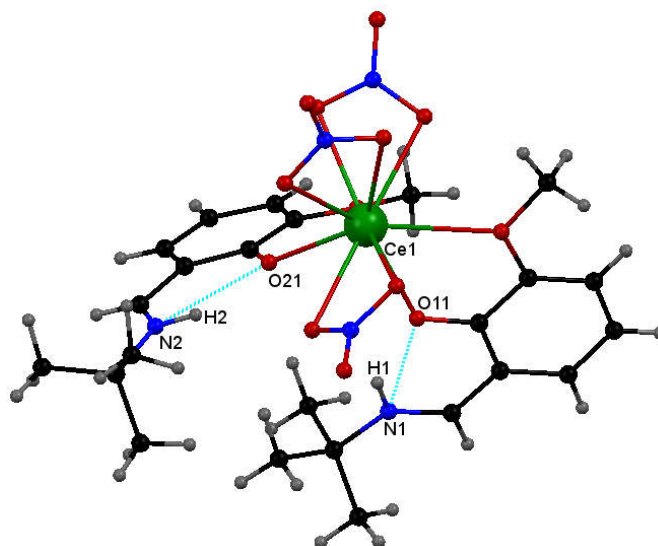


Figure 4f. Hydrogen bonding in complex 1.

The crystal packing of **1** revealed that both intra- and inter-molecular interactions are present in the unit cell of the complex. The inter-molecular interactions are between the uncoordinated methanol molecule and nitrate [ $H6\cdots O33 = 2.5800 \text{ \AA}$ ]. Strong hydrogen bonds between the protonated nitrogen and the phenoxide are present in all the complexes, with  $H\cdots O$  lengths ranging from 1.876(19)–1.97(3)  $\text{\AA}$  and  $N-H\cdots O$  bond angles of 138(3)–142(2) $^\circ$  (Figure 4f; Table 3b).

Table 3b. Hydrogen-bonding geometry ( $\text{\AA}$ ,  $^\circ$ ) for **1**–**5**.

Complex	$D-H\cdots A$	$D-H$	$H\cdots A$	$D\cdots A$	$D-H\cdots A$
Complex 1	N1-H1 $\cdots$ O11	0.85(2)	1.90(2)	2.617(2)	140(2)
	N2-H2 $\cdots$ O21	0.876(19)	1.876(19)	2.609(2)	140.1(18)
	O6-H6 $\cdots$ O33 <sup>i</sup>	0.8400	2.5800	2.902(9)	104.00
Complex 2	N1-H1 $\cdots$ O11	0.85(3)	1.91(3)	2.620(2)	141(2)
	N2-H2 $\cdots$ O21	0.77(3)	1.97(3)	2.611(3)	142(2)
Complex 3	N1-H1 $\cdots$ O11	0.86(4)	1.92(3)	2.623(3)	139(3)
	N2-H2 $\cdots$ O21	0.87(3)	1.88(4)	2.605(3)	139(3)
Complex 4	N1-H1 $\cdots$ O11	0.79(3)	1.95(3)	2.613(3)	141(2)
	N2-H2 $\cdots$ O21	0.89(3)	1.89(3)	2.627(3)	139(2)
Complex 5	N1-H1 $\cdots$ O11	0.81(4)	1.94(4)	2.609(3)	139(3)
	N2-H2 $\cdots$ O21	0.87(4)	1.91(3)	2.628(3)	138(3)

$D$  = donor,  $A$  = acceptor. Symmetry codes: (i) 1-x, 1-y, -z.

## CONCLUSION

A series of mononuclear Ln(III) complexes with the Schiff base ligand 2-((*E*)-(tert-butylimino)methyl)-6-methoxyphenol ( $HL_1$ ) described by general formulae  $[Ce(HL_1)_2(NO_3)_3]\cdot MeOH$  and  $[Ln(HL_1)_2(NO_3)_3]$  ( $Ln = Nd, Gd, Ho$  and  $Er$ ) were isolated and characterized by the usual physico-chemical techniques. The molecular structure of the complexes was confirmed by single-crystal X-ray crystallography. In all the complexes, the Ln(III) ions are ten-coordinate, adopting a tetradecahedron geometry with six oxygen atoms donated by three bidentately coordinated nitrate ions and four oxygen donor atoms from two  $HL_1$ . The  $O, O$ -donor Schiff base ligands in the complexes exist in a zwitterion state. The hydrogen bonds present were mainly between the  $[C=N-H]^+$  moieties and nitrate ions. Additionally, the Ce(III) complex contains one lattice methanol molecule that was found to play an important role in stabilization of the crystal structure through hydrogen bonding with the free oxygen atom of the bidentately coordinated nitrate.

## ACKNOWLEDGEMENTS

Support from the National Research Foundation (unique grant number: 106004) and Nelson Mandela University Postgraduate Research Scholarship is gratefully acknowledged.

### Crystallographic data

Crystallographic data for the reported complexes **1**–**5** have been deposited at the Cambridge Crystallographic Data Centre with CCDC reference numbers 2032529–2032533, respectively. These data are available from the CCDC, 12 Union Road, Cambridge CB2 1EZ, UK on request or can be obtained free of charge from the Cambridge Crystallographic Data Center via <https://www.ccdc.cam.ac.uk/structures>.

## REFERENCES

1. Abo-Aly, M.M.; Salem, A.M.; Sayed, M.A.; Abdel Aziz, A.A. Spectroscopic and structural studies of the Schiff base 3-methoxy-*N*-salicylidene-*o*-amino phenol complexes with some transition metal ions and their antibacterial, antifungal activities. *Spectrochim Acta Part A Mol. Biomol. Spectrosc.* **2015**, *136*, 993–1000.
2. Ebrahimi, H.P.; Hadi, J.S.; Abdulnabi, Z.A.; Bolandnazar, Z. Spectroscopic, thermal analysis and DFT computational studies of salen-type Schiff base complexes. *Spectrochim. Acta Part A Mol. Biomol. Spectrosc.* **2014**, *117*, 485–492.
3. Yu, Y.-Y.; Xian, H.-D.; Liu, J.-F.; Zhao, G.-L. Synthesis, characterization, crystal structure and antibacterial activities of transition metal(II) complexes of the Schiff base 2-[(4-methylphenylimino)methyl]-6-methoxyphenol. *Molecules* **2009**, *14*, 1747–1754.
4. Gao, T.; Yan, P.-F.; Li, G.-M.; Zhang, J.-W.; Sun, W.-B.; Suda, M.; Einaga, Y. Correlations between structure and magnetism of three *N,N'*-ethylene-bis(3-methoxysalicylideneimine) gadolinium complexes. *Solid State Sci.* **2010**, *12*, 597–604.
5. Liao, S.; Yang, X.; Jones, R.A. Self-assembly of luminescent hexanuclear lanthanide salen complexes. *Cryst. Growth Des.* **2012**, *12*, 970–974.
6. Yan, P.-F.; Lin, P.-H.; Habib, F.; Aharen, T.; Murugesu, M.; Deng, Z.-P.; Li, G.-M.; Sun, W.-B. Planar tetranuclear Dy(III) single-molecule magnet and its Sm(III), Gd(III), and Tb(III) analogues encapsulated by salen-type and  $\beta$ -diketonate ligands. *Inorg. Chem.* **2011**, *50*, 7059–7065.
7. Sun, W.-B.; Yan, P.-F.; Li, G.-M.; Zhang, J.-W.; Xu, H. *N,N'*-Bis(3-methoxysalicylidene)propane-1,2-diamine mononuclear 4f and heterodinuclear Cu-4f complexes: Synthesis, crystal structure and electrochemical properties. *Inorg. Chim. Acta* **2009**, *362*, 1761–1766.
8. Zhao, L.; Wu, J.; Keab, H.; Tang, J. Three dinuclear lanthanide(III) compounds of a polydentate Schiff base ligand: Slow magnetic relaxation behaviour of the Dy<sup>III</sup> derivative. *CrystEngComm.* **2013**, *15*, 5301–5306.
9. Yang, X.; Jones, R.A.; Oye, M.M.; Wiester, M.; Lai, R.J. Influence of metal–ligand ratio on benzimidazole based luminescent lanthanide complexes: 3-D network structures and chloride anion binding. *New J. Chem.* **2011**, *35*, 310–318.
10. Moll, O.P.Y.; Borgne, T.L.; Thuéry, P.; Ephritikhine, M. An ion pair uniting a gadolinium(III)-Schiff base complex and uranyl tetrachloride. *Acta Cryst.* **2001**, *C57*, 392–393.
11. Bruker, *APEX 2 & SAINT*, Bruker AXS Inc.: Madison, Wisconsin, USA; **2010**.
12. Spek, A.L. Structure validation in chemical crystallography. *Acta Cryst.* **2009**, *D65*, 148–155.
13. Sheldrick, G.M. A short history of SHELX. *Acta Cryst.* **2008**, *A64*, 112–122.
14. Farrugia, L.J. ORTEP-3 for Windows—A version of ORTEP-III with a graphical user interface (GUI). *J. Appl. Cryst.* **1997**, *30*, 565.
15. Macrae, C.F.; Bruno, I.J.; Chisholm, J.A.; Edgington, P.R.; McCabe, P.; Pidcock, E.; Rodriguez-Mange, L.; Taylor, R.; van de Streek, J.; Wood, P.A. Mercury CSD 2.0 – new features for the visualization and investigation of crystal structures. *J. Appl. Cryst.* **2008**, *41*, 446–470.
16. Geary, W.J. The use of conductivity measurements in organic solvents for the characterisation of coordination compounds. *Coord. Chem. Rev.* **1971**, *7*, 81–122.
17. Sun, W.-B.; Yan, P.-F.; Li, G.-M.; Xu, H.; Zhang, J.-W. *N,N'*-bis(salicylidene)propane-1,2-diamine lanthanide(III) coordination polymers: Synthesis, crystal structure and luminescence properties. *J. Solid State Chem.* **2009**, *182*, 381–388.
18. Gaye, M.; Tamboura, F.B.; Sall, A.S. Spectroscopic studies of some lanthanide(III) nitrate complexes synthesized from a new ligand 2,6-bis-(salicylaldehyde hydrazone)-4-

- chlorophenol. *Bull. Chem. Soc. Ethiop.* **2003**, 17, 27–34.
19. Tai, X.; Wang, H.; Sun, X. Synthesis and spectral characterization of methyl-2-pyridyl ketone benzoyl hydrazone and its complexes with rare earth nitrates. *Spectrosc. Lett.* **2005**, 38, 497–504.
  20. Peters, J.A.; Huskens, J.; Raber, D.J. Lanthanide induced shifts and relaxation rate enhancements. *Prog. Nucl. Magn. Reson. Spectrosc.* **1996**, 28, 283–350.
  21. Singh, B.; Sahai, P.; Singh, P.K. Synthesis and characterization of some lanthanide complexes with 4-acetylpyridine-2-furoylhydrazone. *Synth. React. Inorg. Met.-Org. Chem.* **1998**, 28, 685–697.
  22. Ain, Q.; Pandey, S.K.; Pandey, O.P.; Sengupta, S.K. Synthesis, spectroscopic, thermal and antimicrobial studies of neodymium(III) and samarium(III) complexes derived from tetradentate ligands containing N and S donor atoms. *Spectrochim. Acta Mol. Biomol. Spectrosc.* **2015**, 140, 27–34.
  23. Rao, T.R.; Shrestha, S.; Prasad, A.; Narang, K.K. Synthesis and structural studies of some lanthanide complexes of salicylaldehyde anthranoyl hydrazone. *Synth. React. Inorg. Met.-Org. Chem.* **2002**, 32, 419–436.
  24. Agarwal, R.K.; Prasad, S.; Garg, R.; Sidhu, S.K. Synthesis and preliminary structural characterization of some lanthanide(III) semicarbazone complexes. *Bull. Chem. Soc. Ethiop.* **2006**, 20, 167–172.
  25. Llunell, M.; Casanova, D.; Cirra, J.; Bofill, J.M.; Alcmay, P.; Alvarez, S.; Pinsky, M.; Avnir, D. *SHAPE*, version 2.1, University of Barcelona, Barcelona, Spain, and Hebrew University of Jerusalem: Jerusalem, Israel; **2005**.
  26. Ruiz-Martínez, A.; Alvarez, S. Stereochemistry of compounds with coordination number ten. *Chem. Eur. J.* **2009**, 15, 7470–7480.
  27. Cirera, J.; Ruiz, E.; Alvarez, S. Continuous shape measures as a stereochemical tool in organometallic chemistry. *Organometallics* **2005**, 24, 1556–1562.
  28. Gao, B.; Zhang, Q.; Yan, P.; Hou, G.; Li, G. Crystal engineering of salen type cerium complexes tuned by various cerium counterions. *CrystEngComm.* **2013**, 15, 4167–4175.
  29. Gao, T.; Li, G.-M.; Gao, P.; Yan, P.-F.; Hou, G.-F. [*N,N'*-bis(3-methoxy-2-oxido-benzylidene)ethane-1,2-diaminium- $\kappa^4 O, O', O'', O'''$ ]tris(nitrato- $\kappa^2 O, O'$ )erbium(III). *Acta Cryst.* **2010**, E66, m107.
  30. Shen, J.-B.; Zhao, G.-L. Bis{6-methoxy-2-[(4-methylphenyl)iminomethyl]phenolate- $\kappa^2 O, O'$ }tris(nitrato- $\kappa^2 O, O'$ )holmium(III) monohydrate. *Acta Cryst.* **2010**, E66, m1603–m1604.
  31. Habarurema, G.; Hosten, E.C.; Gerber, T.I.A. Coordination of a Schiff base as an iminium-phenone zwitterion in a double ligand-bridged *fac*-[Re(CO)<sub>3</sub>]<sup>+</sup> dimer. *Inorg. Chem. Commun.* **2015**, 60, 23–26.
  32. Armelao, L.; Quici, S.; Barigelletti, F.; Accorsi, G.; Bottaro, G.; Cavazzini, M.; Tondello, E. Design of luminescent lanthanide complexes: From molecules to highly efficient photo-emitting materials. *Coord. Chem. Rev.* **2010**, 254, 487–505.
  33. Ishida, T.; Watanabe, R.; Fujiwara, K.; Okazawa, A.; Kojima, N.; Tanaka, G.; Yoshiie, S.; Nojiri, H. Exchange coupling in TbCu and DyCu single-molecule magnets and related lanthanide and vanadium analogs. *Dalton Trans.* **2012**, 41, 13609–13619.